

A NOVEL High Step-Up Converter with a Voltage Multiplier Module for a Photovoltaic System

A.Narasimhulu¹, Dr.C.Narayana Reddy²PG Student [PE&ED], Dept. of EEE, SV Engineering College, Chittoor, Andhra Pradesh, India¹Professor, Dept of EEE, SVCET, Chittoor, Andhra Pradesh, India²

ABSTRACT: A novel high step-up converter is proposed for a front end photovoltaic system. Through a voltage multiplier module, an asymmetrical interleaved high step-up converter usually high step up gain without act as a function at an extreme duty ratio. The voltage multiplier module is create of a conventional boost converter and coupled inductors. An extra conventional boost converter is combine into the first phase to achieve a considerably higher voltage conversion ratio. The two-phase configuration not only decreases the current stress through each power switch, but also force to do some thing the input current ripple, which decreases the conduction losses of metal–oxide–semiconductor field-effect transistors (MOSFETs). In addition, the proposed converter functions as an active clamp circuit, which moderate large voltage spikes across the power switches. Thus, the low-voltage-rated MOSFETs can be adopted for reduces of conduction losses and cost. Efficiency improves because the energy stored in leakage inductances is energized to the output terminal. Finally, the prototype circuit with a 40-V input voltage, 380-V output, and 1000- W output power is operated to verify its performance. The highest efficiency is 96.8%.

KEY WORDS: High Step-up Converter, Voltage Multiplier module, Boost Converter, photovoltaic system

I.INTRODUCTION

Renewable sources of energy are increasingly valued worldwide because of energy shortage and environmental contamination. Renewable energy systems generate low voltage output; thus, high step-up dc/dc converters are widely employed in many renewable energy applications, including fuel cells, wind power, and photovoltaic systems . Among renewable energy systems, photovoltaic systems are expected to play an important role in future energy production . Such systems transform light energy into electrical energy, and convert low voltage into high voltage via a step-up converter, which can convert energy into electricity using a grid-by-grid inverter or store energy into a battery set. Fig. 1 shows a typical photovoltaic system that consists of a solar module, a high step up converter, a charge-discharge controller, a battery set, and an inverter.

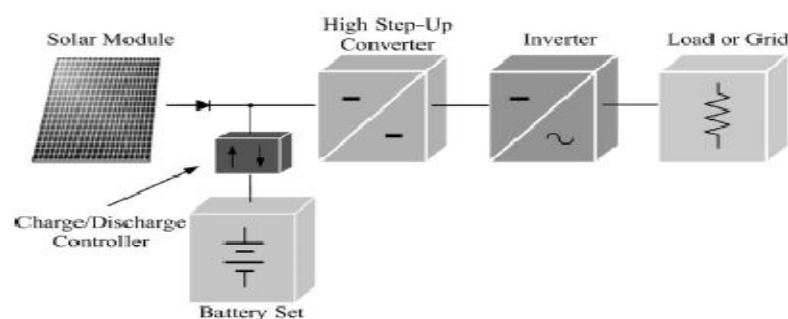


Figure1: Typical photovoltaic system

The high step-up converter performs importantly among the system because the system requires a sufficiently high step-up conversion. Theoretically, conventional step-up converters, such as the boost converter and fly back converter, cannot achieve a high step-up conversion with high efficiency because of the resistances of elements or leakage inductance. Thus, a modified boost–fly back converter was proposed, and many converters that use the coupled inductor for a considerably high voltage conversion ratio were also proposed.

International Journal of Advanced Research in Electrical, Electronics and Instrumentation Engineering

(An ISO 3297: 2007 Certified Organization)

Vol. 3, Issue 11, November 2014

II. LITERATURE SURVEY

Conventional step-up converters, such as the boost converter and fly back converter, cannot achieve a high step-up conversion with high efficiency because of the resistances of elements or leakage inductance. Conventional step-up converters with a single switch are unsuitable for high-power applications given an input large current ripple, which increases conduction losses.

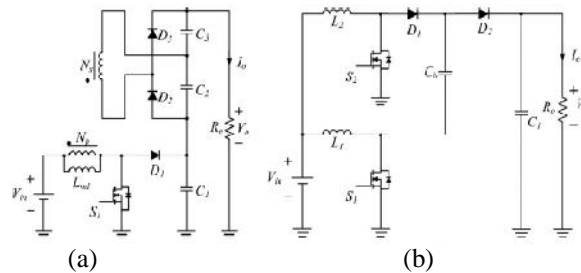


Figure 2: High step-up techniques based on a classical boost converter. (a) Integrated fly back–boost converter structure. (b) Interleaved boost converter with a voltage-lift capacitor structure

Thus, numerous interleaved structures and some asymmetrical interleaved structures are extensively used. The current study also presents an asymmetrical interleaved converter for a high step-up and high-power application. Modifying a boost–fly back Converter. One of the simple approaches to achieving high step-up gain; this gain is realized via a coupled inductor. The performance of the converter is similar to an active-clamped fly back converter; thus, the leakage energy is recovered to the output terminal.

III. PROPOSED SYSTEM

It obtains extra voltage gain through the voltage-lift capacitor, and reduces the input current ripple, which is suitable for power factor correction (PFC) and high-power applications. In this paper, an asymmetrical interleaved high step-up converter that combines the advantages of the aforementioned converters is proposed, which combined the advantages of both. In the voltage multiplier module of the proposed converter, the turns ratio of coupled inductors can be designed to extend voltage gain, and a voltage-lift capacitor offers an extra voltage conversion ratio. The advantages of the proposed converter are as follows:

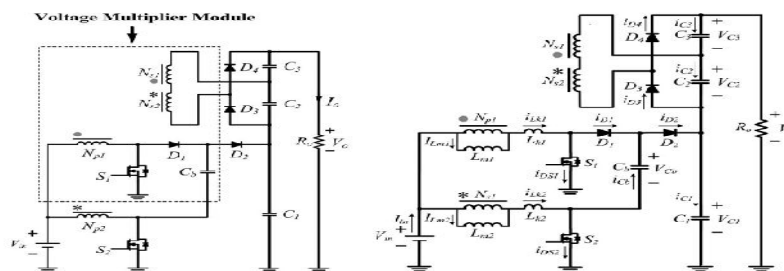


Figure: 3 (a) proposed high step-up converter with a voltage multiplier module. (b) Equivalent circuit of the proposed converter.

- 1) the converter is characterized by a low input current ripple and low conduction losses, making it suitable for high power applications;
- 2) The converter achieves the high step-up voltage gain that renewable energy systems require;
- 3) Leakage energy is recycled and sent to the output terminal, and alleviates large voltage spikes on the main switch;
- 4) The main switch voltage stress of the converter is substantially lower than that of the output voltage;
- 5) Low cost and high efficiency are achieved by the low $rDS(on)$ and low voltage rating of the power switching device.

International Journal of Advanced Research in Electrical, Electronics and Instrumentation Engineering

(An ISO 3297: 2007 Certified Organization)

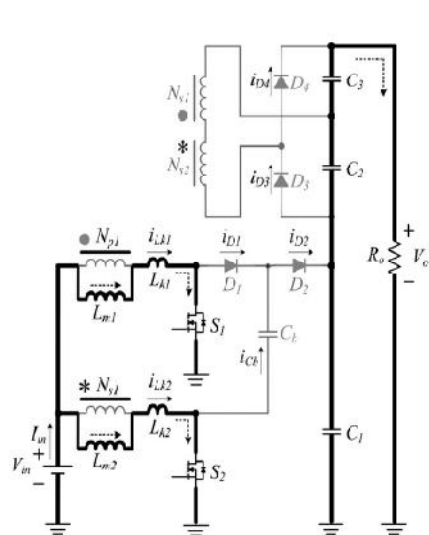
Vol. 3, Issue 11, November 2014

A) OPERATING PRINCIPLE DESCRIPTION:

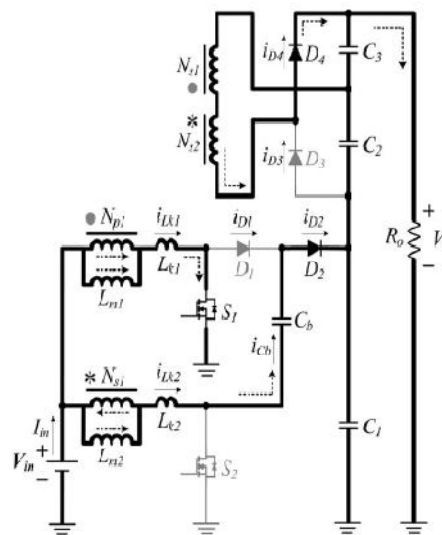
The proposed high step-up converter with voltage multiplier module is shown in Fig. 3(a). A conventional boost converter and two coupled inductors are located in the voltage multiplier module, which is stacked on a boost converter to form an asymmetrical interleaved structure. Primary windings of the coupled inductors with Np turns are employed to decrease input current ripple, and secondary windings of the coupled inductors with Ns turns are connected in series to extend voltage gain. The turns ratios of the coupled inductors are the same. The coupling references of the inductors are denoted by “.” and “*” in Fig. 3.

The equivalent circuit of the proposed converter is shown in Fig. 3(b), where $Lm1$ and $Lm2$ are the magnetizing inductors, $Lk1$ and $Lk2$ represent the leakage inductors, $S1$ and $S2$ denote the power switches, Cb is the voltage-lift capacitor, and n is defined as a turns ratio Ns/Np .

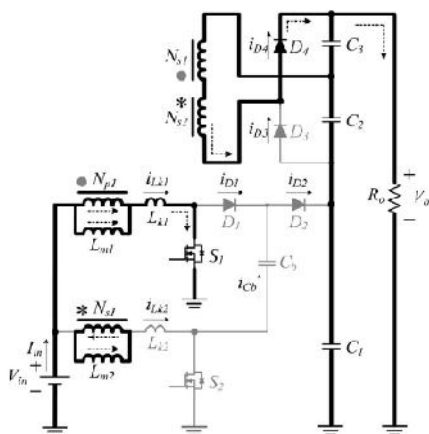
The proposed converter operates in continuous conduction mode (CCM), and the duty cycles of the power switches during steady operation are inter leaved with a 180° phase shift; the duty cycles are greater than 0.5. The key steady waveforms in one switching period of the proposed converter contain six modes, which are depicted in Fig shows the topological stages of the circuit.



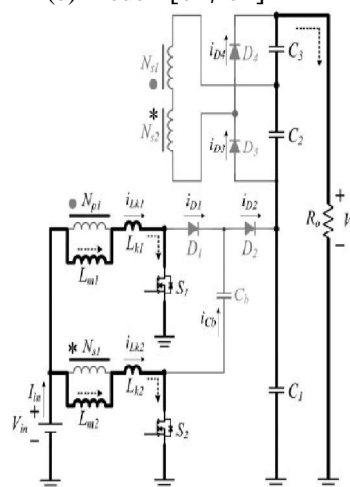
(a) Mode-1 [t_0, t_1].



(b) Mode-2 [t_1, t_2]



(c) Mode-3 [t_2, t_3].

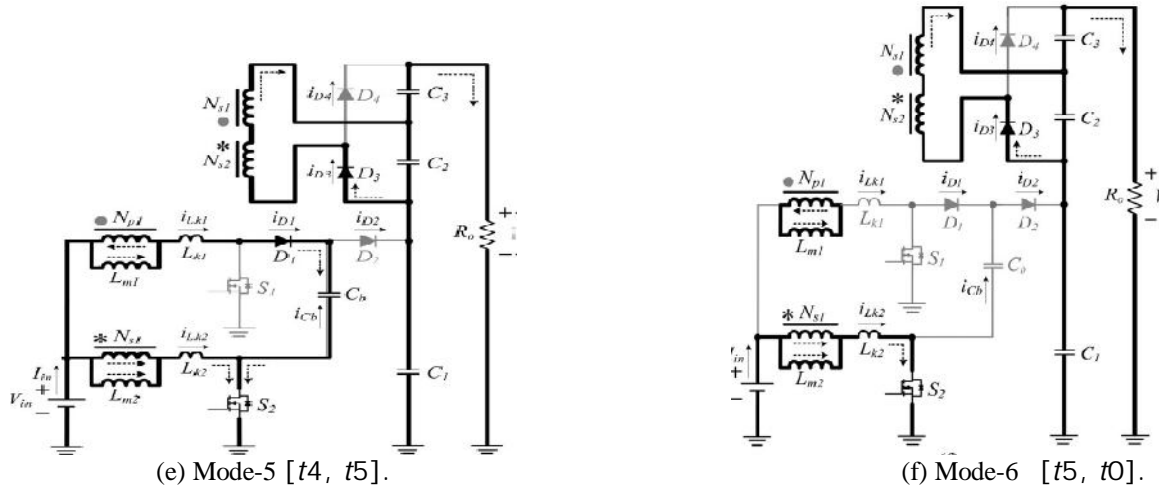


(d) Mode-4 [t_3, t_4].

International Journal of Advanced Research in Electrical, Electronics and Instrumentation Engineering

(An ISO 3297: 2007 Certified Organization)

Vol. 3, Issue 11, November 2014



Mode 1 [t0, t1]: At $t=t_0$, the power switches S_1 and S_2 are both turned ON. All of the diodes are reversed-biased. Magnetizing inductors L_{m1} and L_{m2} as well as leakage inductors L_{k1} and L_{k2} are linearly charged by the input voltage source V_{in} .

Mode 2 [t1, t2]: At $t=t_1$, the power switch S_2 is switched OFF, thereby turning ON diodes D_2 and D_4 . The energy that magnetizing inductor L_{m2} has stored is transferred to the secondary side charging the output filter capacitor C_3 . The input voltage source, magnetizing inductor L_{m2} , leakage inductor L_{k2} , and voltage-lift capacitor C_b release energy to the output filter capacitor C_1 via diode D_2 , thereby extending the voltage on C_1 .

Mode 3 [t2, t3]: At $t=t_2$, diode D_2 automatically switches OFF because the total energy of leakage inductor L_{k2} has been completely released to the output filter capacitor C_1 . Magnetizing inductor L_{m2} transfers energy to the secondary side charging the output filter capacitor C_3 via diode D_4 until t_3 .

Mode 4 [t3, t4]: At $t=t_3$, the power switch S_2 is switched ON and all the diodes are turned OFF. The operating states of modes 1 and 4 are similar.

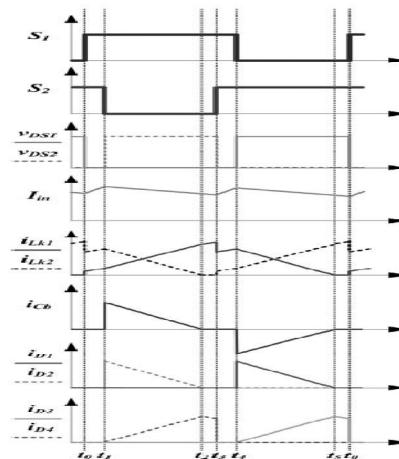


Figure 4: Steady waveforms of the proposed converter at CCM.

Mode 5 [t4, t5]: At $t=t_4$, the power switch S_1 is switched OFF, which turns ON diodes D_1 and D_3 . The energy stored in magnetizing inductor L_{m1} is transferred to the secondary side charging the output filter capacitor C_2 . The input voltage source and magnetizing inductor L_{m1} release energy to voltage-lift capacitor C_b via diode D_1 , which stores extra energy in C_b .

Mode 6 [t5, t0]: At $t=t_5$, diode D_1 is automatically turned OFF because the total energy of leakage inductor L_{k1} has been completely released to voltage-lift capacitor C_b . Magnetizing inductor L_{m1} transfers energy to the secondary side charging the output filter capacitor C_2 via diode D_3 until t_0 .

International Journal of Advanced Research in Electrical, Electronics and Instrumentation Engineering

(An ISO 3297: 2007 Certified Organization)

Vol. 3, Issue 11, November 2014

IV CONVERTER COMPONENTS AND PARAMETERS

Components	Symbols	Parameters
Magnetizing inductances	L_{m1}, L_{m2}	133 μ H
Leakage inductances	L_{k1}, L_{k2}	1.6 μ H
Turns ratio	$n(N_s, N_p)$	1
Power switches	S_1, S_2	IRFP4227
Diodes	D_1, D_2, D_3	FCF06A-40 BY Q28E-200
Capacitance	C_b, C_2, C_3, C_1	200 μ f, 470 μ f

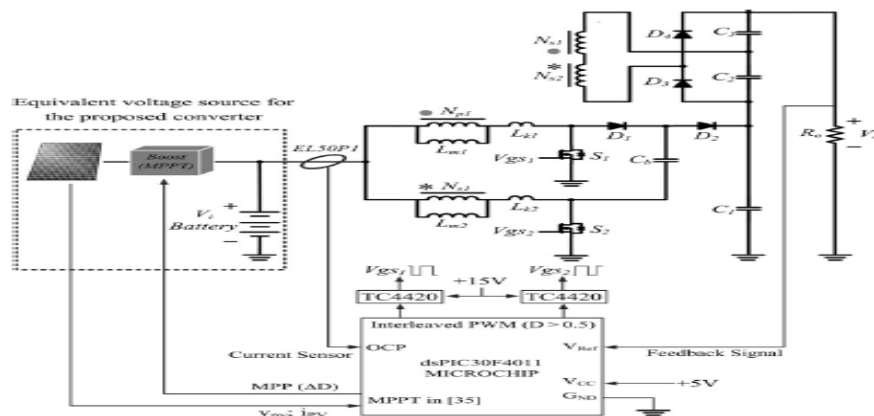


Figure-5: Control strategy for the proposed converter.

The high step-up interleaved converter introduced in is also suitable as a candidate for high step-up, high-power conversion of the PV system, and the other high step-up interleaved converter introduced in , which is an asymmetrical interleaved structure as proposed converter is favourable for dc-micro grid applications. Both of converters use coupled inductor and voltage double to achieve high step-up conversion. For the proposed converter, the step-up gain is highest and the voltage stress on switch is the lowest, as converter introduced. Under the turns ratio n designed as less than 2, the highest voltage stress on diodes of the proposed converter is the lowest among the compared converters. In addition, the quantities of diodes are the least as converter introduced .Because the components of the proposed converter are the least among the compared converters, the reliability is higher and the cost is lower. Thus, the proposed converter is suitable for high step-up, high-power applications such as PV system.

In control strategy, the proposed converter is controlled by the microchip dsPIC30F4011 as shown in Fig. 5 PV module and battery set are the main input power sources, which can be seen as an equivalent voltage source for the proposed converter, and the MPPT algorithm is employed by referring . The battery management system (BMS) for the charge/discharge controller is not the main priority in this paper; thus, the related designed is not implemented in the paper.

V. DESIGN AND EXPERIMENTAL RESULTS

A prototype of the proposed high step-up converter with a40-V input voltage, 380-V output voltage, and maximum output power of 1 kW is tested. The switching frequency is 40 kHz, and the corresponding component parameters are listed in Table II for reference .The design consideration of the proposed converter includes component selection and coupled inductors design, which are based on the analysis presented in the previous section. In the proposed converter, the values of the primary leakage inductors of the coupled inductors are set as close as possible for

International Journal of Advanced Research in Electrical, Electronics and Instrumentation Engineering

(An ISO 3297: 2007 Certified Organization)

Vol. 3, Issue 11, November 2014

current sharing performance. Due to the performances of high step-up gain, the turns ratio n can be set 1 for the prototype circuit with a 40- V input voltage, 380- V output to reduce cost, volume, and conduction loss of winding. Thus, the copper resistances which affect efficiency much can be decreased.

A) Simulation circuit and Results:

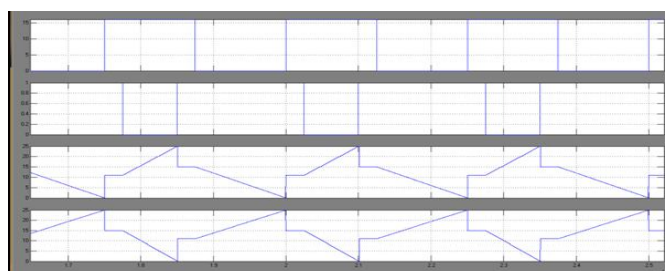
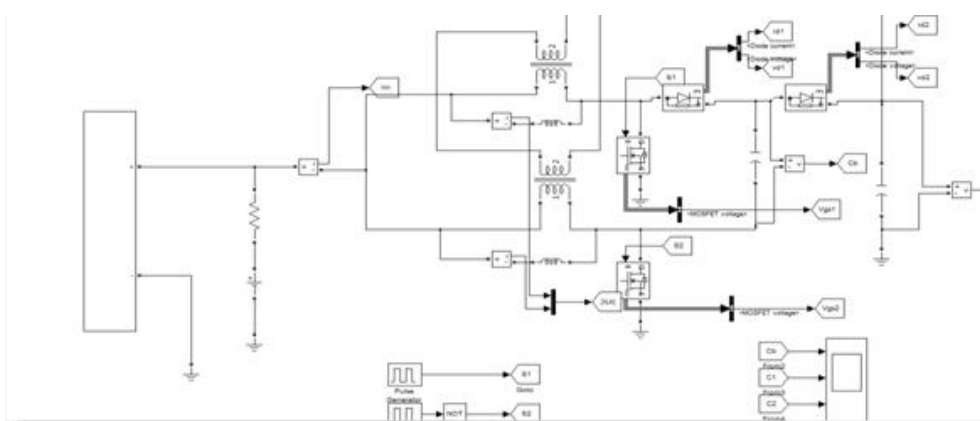


Figure 6(a): Results for $V_{gs1}, V_{gs2}, I_{Lk1}$ and I_{Lk2}

Fig.6(a) illustrates the measured waveforms of $V_{gs1}, V_{gs2}, i_{Lk1}, i_{Lk2}, V_{ds1}, V_{ds2}$ and i_{ls} at $P_o = 1$ kW. In Fig. 6, the switch voltage is clamped at 90 V, which is much smaller than the output voltage 380 V. Fig. 6(b) illustrate the Measured waveforms of $V_{gs1}, V_{gs2}, i_{D1}, i_{D2}, i_{D3}$, and i_{D4} at $P_o = 1$ kW. The measured waveforms are consistent with the steady-state analysis.

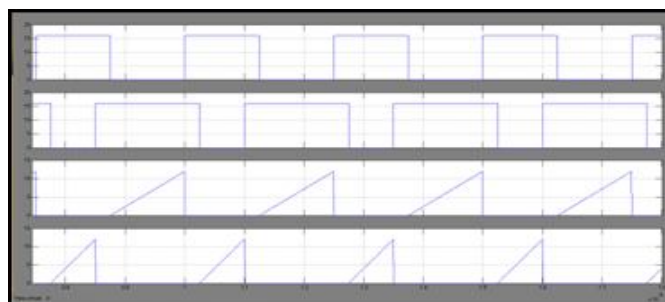


Figure 6(b):Results for $v_{gs1}, v_{gs2}, i_{d3}, i_{d4}$

Fig. 6(b) illustrate the Measured waveforms of $V_{gs1}, V_{gs2}, i_{D1}, i_{D2}, i_{D3}$, and i_{D4} at $P_o = 1$ kW. The measured waveforms are consistent with the steady-state analysis.

International Journal of Advanced Research in Electrical, Electronics and Instrumentation Engineering

(An ISO 3297: 2007 Certified Organization)

Vol. 3, Issue 11, November 2014

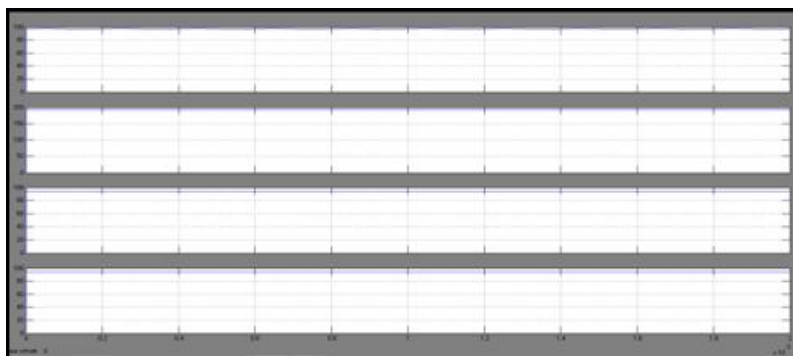


Figure 7 : Results for high – Voltage Storage of Capacitor

Fig. 7 shows the simulation and experimental result of voltage on all capacitor to illustrate the high voltage storage and theoretical analysis. V_{c1} is equal to V_{cb} plus output voltage of boost converter, and V_{cb} is equal to the output voltage of the boost converter. Thus, V_{c1} is twice of V_{cb} . V_{c2} is equal to V_{c3} ; both are nearly V_{cb} because turns ratio n is set 1.

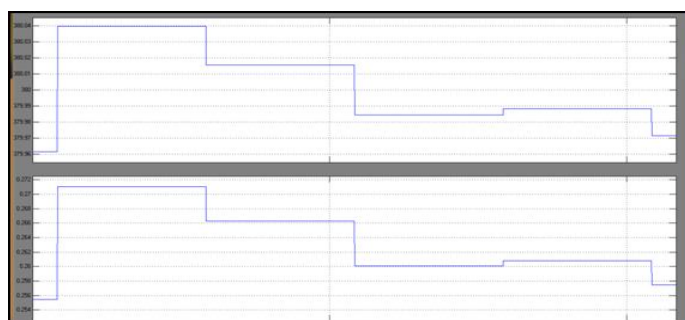


Figure 8 : Results for Dynamic Response under Step load

Fig.8 shows the input current ripple i_{in} and the currents i_{LK1} and i_{LK2} the primary side of the coupled inductors at $P_o = 1$ kW. The peak-to-peak current ripple is about 2 A (6%), which confirms that the input current ripple is very low even if at high-power operation.

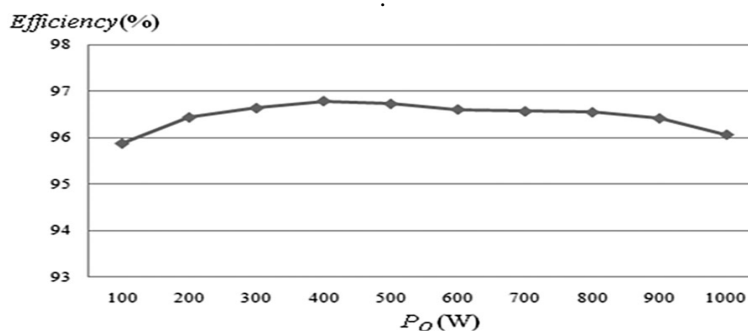


Figure 9: Measured efficiency of the proposed converter.

Figure 9: shows the measured efficiency of the proposed converter. The maximum efficiency is 96.8% at $P_o = 400$ W. At maximum output power, the conversion efficiency is about 96.1%.



International Journal of Advanced Research in Electrical, Electronics and Instrumentation Engineering

(An ISO 3297: 2007 Certified Organization)

Vol. 3, Issue 11, November 2014

VI.CONCLUSION

This paper has presented the topological principles, steady state analysis, and experimental results for a proposed converter. The proposed converter has been successfully implemented in an efficiently high step-up conversion without an extreme duty ratio and a number of turns ratios through the voltage multiplier module and voltage clamp feature. The interleaved PWM scheme reduces the currents that pass through each power switch and constrained the input current ripple by approximately 6%. The experimental results indicate that leakage energy is recycled through capacitor C_b to the output terminal. Meanwhile, the voltage stresses over the power switches are restricted and are much lower than the output voltage (380 V). These switches, conducted to low voltage rated and low on-state resistance MOSFET, can be selected. Furthermore, the full-load efficiency is 96.1% at $P_o = 1000$ W, and the highest efficiency is 96.8% at $P_o = 400$ W. Thus, the proposed converter is suitable for PV systems or other renewable energy applications that need high step-up high-power energy conversion.

REFERENCES

- [1] C. Hua, J. Lin, and C. Shen, "Implementation of a DSP-controlled photovoltaic system with peak power tracking," *IEEE Trans. Ind. Electron.*, vol. 45, no. 1, pp. 99–107, Feb. 1998.
- [2] J. M. Carrasco, L. G. Franquelo, J. T. Bialasiewicz, E. Galvan, R. C. P. Guisado, M. A. M Prats, J. I. Leon, and N. Moreno-Alfonso, "Power-electronic systems for the grid integration of renewable energy sources: A survey," *IEEE Trans. Ind. Electron.*, vol. 53, no. 4, pp. 1002– 1016, Jun. 2006.
- [3] J. T. Bialasiewicz, "Renewable energy systems with photovoltaic power generators: Operation and modeling," *IEEE Trans. Ind. Electron.*, vol. 55, no. 7, pp. 2752–2758, Jul. 2008.
- [4] Y. Xiong, X. Cheng, Z. J. Shen, C. Mi, H.Wu, and V. K. Garg, "Prognostic and warning system for power-electronic modules in electric, hybrid electric, and fuel-cell vehicles," *IEEE Trans. Ind. Electron.*, vol. 55, no. 6, pp. 2268–2276, Jun. 2008.
- [5] F. S. Pai, "An improved utility interface for micro-turbine generation system with stand-alone operation capabilities," *IEEE Trans. Ind. Electron.*, vol. 53, no. 5, pp. 1529–1537, Oct. 2006.
- [6] H. Tao, J. L. Duarte, and M. A. M. Hendrix, "Line-interactive UPS using a fuel cell as the primary source," *IEEE Trans. Ind. Electron.*, vol. 55, no. 8, pp. 3012–3021, Aug. 2008.
- [7] Z. Jiang and R. A. Dougal, "A compact digitally controlled fuel cell/battery hybrid power source," *IEEE Trans. Ind. Electron.*, vol. 53, no. 4, pp. 1094–1104, Jun. 2006.